Front. Earth Sci.
https://doi.org/10.1007/s11707-022-1072-4

RESEARCH ARTICLE

Tree ring derived summer temperature variability over the past millennium in the western Himalayas of northern Pakistan

Fayaz ASAD (✉)[1], Haifeng ZHU[2,3], Tabassum YASEEN[1], Ru HUANG[2], Mukund Palat RAO[4,5,6]

1 Department of Botany, Bacha Khan University Charsadda, Khyber Dakhtun Khaw 24420, Pakistan
2 State Key Laboratory of Tibetan Plateau Earth System, Resources and Environment (TPESRE), Institute of Tibetan Plateau Research, Chinese Academy of Sciences, Beijing 100101, China
3 China Pakistan Joint Research Center on Earth Sciences, CAS-HEC, Islamabad 45320, Pakistan
4 Centre de Recerca Ecològica i Aplicacions Forestals, Barcelona 08193, Spain
5 Department of Plant Science, University of California Davis (UC Davis) 95616, California, USA
6 Tree Ring Laboratory, Lamont-Doherty Earth Observatory, Columbia University, NY 10964, USA

© Higher Education Press 2023

Abstract Long-term high resolution climate proxies are essential for understanding climate variability particularly, in regions such as the western Himalayas of northern Pakistan, where few long-term climate records are available. Using standard dendrochronological methods, an 1132-year (882 to 2013 C.E.) tree-ring chronology of *Juniperus excelsa* M. Bieb was established from the western Himalayas, northern Pakistan (WHNP). Tree growth was negatively and significantly (r = −0.65) correlated with the growing season (June–July) mean temperature, and positively and weakly (r = 0.22) associated with precipitation. This inverse relationship of tree radial growth with temperature and positive association with precipitation demonstrated that forest growth is sensitive to high temperature related drought. Utilizing a reliable STD chronology and robust reconstruction model, a 928-year (1086 to 2013 C.E.) mean temperature reconstruction was developed for the WHNP using the substantial negative correlation between the summer temperature and standard tree ring-width chronology. According to statistical validation, the reconstruction accounted for 41.6% of the climatic variation for the period of 1956–2013 C.E. instrumental period. Individual extreme-warm periods occurred in 1093 C.E. (29.42°C) and extreme cold periods in 1088 C.E. (26.99°C) observed during the past 928 years. The reconstruction's multi-taper method (MTM) spectral analysis reveals significant (p < 0.05) 2–3-year and 63.8-year cycles. Since the 2–3-year cycle occurred within the range of ENSO variation, which indicates that ENSO had an impact on the regional temperature in our studied area.

Keywords tree rings, *Juniperus excelsa*, dendrochronology, reconstruction, western Himalaya

Received October 26, 2022; accepted April 10, 2023

E-mail: fayaz.asad79@gmail.com

1 Introduction

With its extremely susceptible alpine ecosystem and rapidly expanding human population, the Western Himalayan region in Northern Pakistan is one of the region's most at risk from climate change (Khan et al., 2021). This region is also the freshwater tower of South Asia and is part of the Third Pole region (Zhang et al., 2019). Due to its unique topography, it is often referred to as a climate-sensitive "hotspot" in Pakistan (Hewitt, 2002). More broadly, the Himalayan region has been experiencing adverse environmental impacts due to rapidly rising temperatures (Sabin et al., 2020). Studies have revealed that global warming is substantially reducing the mass of glaciers in the Himalayan area (Kargel et al., 2011; Bolch et al., 2012; Cogley, 2012; Shekhar et al., 2017). Over the previous few decades, according to a regional-based climate reconstruction data set, the Karakoram-Himalayas has not warmed significantly in contrast to rising trend in temperature across the northern Hemisphere (Zafar et al., 2016). Hence, it important to understand the long-term climatic variability (for past millennium) in the western Himalayan region contextualise regional changes relative to global climate change. The network of instrumental

meteorological stations in the WHNP are sparsely distributed and relatively short. They generally do not extend prior to the 1950s making it hard to comprehensively investigate low-frequency and long-term (centennial to decadal) climatic variability in the WHNP (from 1955 C.E.) (Huang et al., 2019a).

Climatic proxies, such as tree rings, can however be used to fill this gap (Fritts, 1976). Tree rings have been frequently utilized to reconstruct historical climatic variations in the Tibetan Plateau (Huang and Zhang, 2007; Liang et al., 2008; Liang et al., 2009; Zhu et al., 2011; Lv and Zhang, 2013; Liang et al., 2016; Tao et al., 2021); Nepal (Cook et al., 2003; Chhetri, 2008; Borgaonkar et al., 2020; Gaire et al., 2020); Tajikistan (Opała-Owczarek et al., 2017; Opała et al., 2017), and Karakoram-Himalayas northern Pakistan (Esper, 2000; Esper et al., 2002; Treydte et al., 2006; Esper et al., 2007; Zafar et al., 2016; Asad et al., 2017; Zhu et al., 2021; Huang et al., 2022). These reconstructions based on tree-ring chronologies can assist in providing a better understanding of regional climatic variability (Liang et al., 2008). Tree-ring-based temperature studies in northern Pakistan, which typically cover the past 500 years and have predominantly focused on temperature change in the Karakoram region using either maximum latewood density or tree-ring width (TRW) chronologies (Zafar et al., 2016; Asad et al., 2017; Huang et al., 2022). However, there are very few studies on the historical temperature change over a period of five centuries in the WHNP region (Khan et al., 2021). Hence, the trajectory of temperature change in this region during the last millennium is not fully understood, particularly the low-frequency temperature fluctuations. This knowledge can also be used to understand the current warming trends to compare with the other regional trends of the Karakoram and Himalaya of northern Pakistan.

Therefore, the objectives of this research were to (i) construct the oldest TRW chronologies from *Juniperus excelsa* on the WHNP and (ii) reconstruct the temperature variation in the WHNP during the past millennium for the study region.

2 Materials and methods

2.1 Study area and climate

The study area is located in northern Pakistan (Fig. 1), which consists of high mountains and is one of the few heavily glaciated regions outside the polar regions (Kamp and Owen, 2011). The mountain system stretches from the east-southeast to the west-northwest in a curved shape, covering a distance of 2400 km (Khan et al., 2021). The Western Himalayas have long been a physical and cultural barrier between South and Central Asia, covering Kashmir and the northern part of Pakistan. Generally, all the major rivers and their tributaries originating from these mountainous regions receive water from the glaciers and snow-covered mountains (Immerzeel et al., 2009; Kumar et al., 2015).

The climate in the Himalayas of northern Pakistan varies enormously depending on the topography and elevation (Bishop et al., 2002). The majority of the region is arid and semi-arid (Ahmed et al., 2018), with the exception of the sub-mountainous region and the southern slopes of the Himalayas, where annual rainfall range is 760–1270 mm. The climate in this region is subtropical humid. A highland climate predominates in the extreme north due to enormous heights (e.g., Fowler and Archer, 2006). Regional averages of the Bunji instrumental weather station close to the sampling location from 1956 to 2013 C.E. show that the average yearly temperature is 17.67°C and that the average total annual precipitation is around 157.17 mm. The months of March and May have

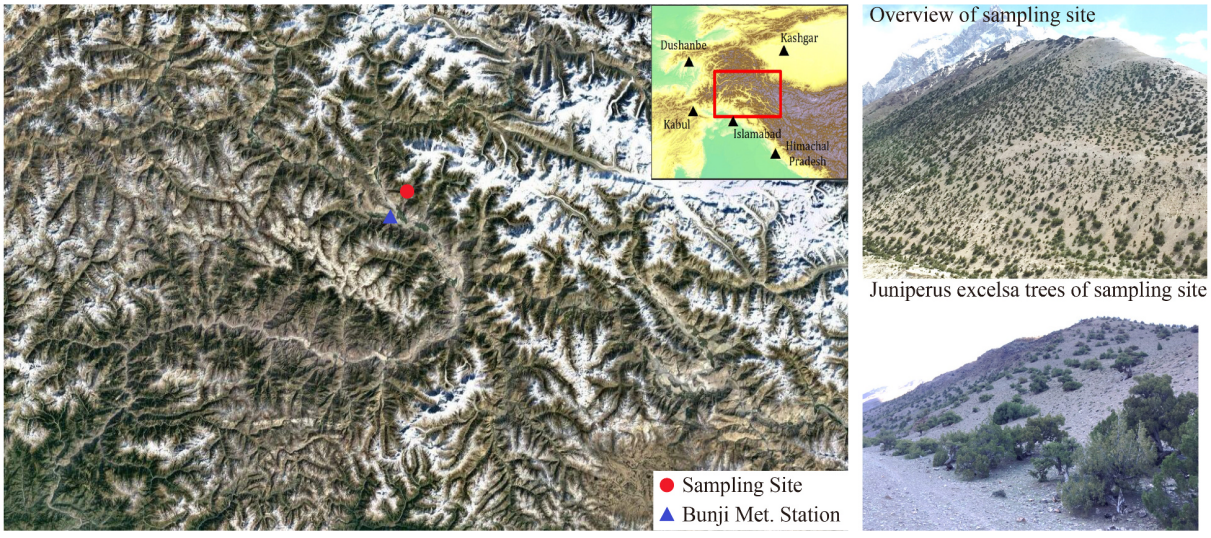

Fig. 1 Tree-ring sampling site, meteorological station and overview of the sampling area used in this study.

the highest reported precipitation, whereas November and December have the lowest. The January (5.04°C) and July (29.16°C) are the warmest and coldest months, respectively (Fig. 2). The study area is typically an arid and semi-arid environment with a cold winter, a wet spring, and a dry and warm summer.

2.2 Tree-ring sampling and chronology development

In the dry and harsh climatic conditions of Pakistan, juniper trees and the diversity of associated plants and animals make up a distinct ecosystem (Sarangzai et al., 2012). In Baluchistan and the inner drier Himalayan valleys between 2000 and 4000 m, *Juniperus excelsa* is very widespread, forming open forests. In May 2017, the tree-ring cores were collected at 3798–3890 m in the Boibar avgrach region in the Himalayas northern Pakistan (Table 1). The sampling region is free from any disturbance or anthropogenic activity. At breast height, at least two increment cores were obtained from a total of 30 healthy trees (total of 60 increment cores). Every tree-ring sample was processed using standard dendrochronological technique (Fritts, 1976; Cook and Briffa, 1990). Tree ring samples were air-dried at room temperature, affixed to wood mounts, sanded using successively thinner sandpaper, cross-dated, and their ring width was measured using the LINTAB-6 with a precision of 0.01 mm. The accuracy of the cross-dating and TRW assessment were examined using the COFECHA program (Holmes, 1983).

We commonly applied variance stabilization routine incorporated into the program ARSTAN (Cook, 1985) to determine ratios between the raw measurement series and negative exponential functions in order to retain low-frequency climatic signals in the final TRW chronology (Cook and Kairiukstis, 1990). We averaged the detrended series to produce a standard mean chronology (Fig. 3). The statistical characteristics of this chronology showed that the expressed population signal (Eps) and running average correlation among series (Rbar), the most reputable and representative time period of the chronology (Fritts, 1976). Rbar denotes the intensity of the tree-ring chronology signal, whereas EPS can indicate how well a chronology reflects a theoretically infinite population based on a finite sample size. EPS > 0.85 is the accepted cutoff (Wigley et al., 1984) (Table 1). Therefore, we believe that 1086–2013 C.E. is the most reliable period, where the sample depth of 10 cores is when the criterion of 0.85 is achieved.

2.3 Climate data and its relationship to trees growth

The analysis of Pearson's correlation was used to assessed the trees growth relationship with climate variables, utilizing the STD chronology and climate factors from nearby meteorological station of Bunji e.g., (Fritts, 1976; Zhu et al., 2011). The climate factors included monthly mean, maximum and minimum temperatures and monthly total precipitation of 1956–2013 C.E. e.g. (Asad et al., 2017). Pearson correlations were evaluated using the climatic data from the prior year's February to the current year's September in view of the climate in the year previous to tree-ring formation may have an effect on tree growth (Fritts, 1976).

2.4 Reconstruction of the climate and statistics

The basic linear regression approach was used to generate the regression model. Split-period of calibration and verification analysis was used to evaluate the reliance of the regression model (Fritts, 1976). Statistics of the split interval of calibration and verification investigation include Pearson's coefficient of correlation (r), Adjusted explained variance (Adj R^2) explained variance (R^2), sign tests (ST) and reduction of error (RE). To assess our reconstruction's spatial representativity, we also estimated spatial correlations between it and the CRU TS 4.05 June to July mean temperature field from 1955 to 2012 using the KNMI climate explorer (available at WMO website).

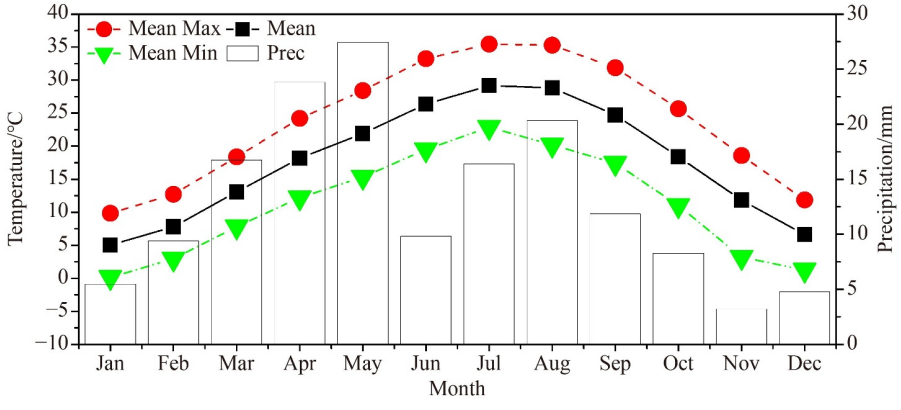

Fig. 2 Bunji meteorological stations include monthly mean maximum (red lines with arrows), mean minimum (green lines with arrows), and mean (black lines with arrows) temperatures and precipitation (white bars).

Table 1 Statistics and site information for the TRW chronology

Study area	Boibar Avgrach Valley Himalayas
Tree species	*Juniperus excelsa*
Latitude	36.625°
Longitude	74.939°
Altitude/m	3798–3890
Cores and trees	60 cores from 30 trees
Time span	882–2013
Mean sensitivity	0.28
Average correlation between all series (r1)	0.37
Average correlation between trees (r2)	0.36
Signal to noise ratio (SNR)	30.01
Expressed population signal (EPS)	0.98

3 Results and discussion

3.1 Characteristics of TRW chronology

We developed a well replicated 1132-year (882 to 2013 C.E.) STD chronology of *Juniperus excelsa* from the north-western Himalayas of Pakistan (Fig. 3). TRW chronology has fluctuated over the mean (0.99). The chronology is reliable to reflect the corresponding population after 1086 C.E. based on the EPS threshold limit (EPS 0.85) (Fig. 3). Positive growth phases were observed for the periods of 1117–1136, 1145–1167, 1220–1232, 1238–1254, 1303–1325, 1303–1325, 1362–1372, 1399–1410, 1461–1473, 1485–1509, 1538–1548, 1561–1572, 1586–1600, 1731–1742, 1792–1817, 1888–1898, 1900–1911, 1936–1962, 1981–2000, and 2000–2013 C.E.. On the other hand, low growth phases were observed between 1276–1292, 1344–1361, 1437–1451, 1604–1618, 1630–1600, 1636–1688, 1705–1718, 1147–1777, 1832–1856, 1859–1868, 1910–1921, and 1963–1980 C.E..

The standard deviation and mean sensitivity of the chronology is relatively high, whereas the average correlation between all series was 0.37, the mean correlation between trees was 0.36, the signal-to-noise ratio was 30.01, and the total missing rings was 135 (0.31%). It was believed that autocorrelation, which illustrates how the growth of the current year depends on the growth of the prior year was reliable for recreating the previous temperature. The *Juniperus excelsa* tree-ring width chronology has a significant common signal, likely attributable to a shared climate signal, as indicated by the high mean series inter-correlation (Table 1).

3.2 Analysis of climate tree growth relationships

The correlation between the ring width indices (RWI) and monthly climate data over the period of 1956–2013 C.E. are calculated (Fig. 4). Only the months of June and July show a significant negative connection ($p < 0.001$) with temperature variables (monthly maximum (T_{max}), minimum (T_{min}), and mean (T_{mean}) temperatures). Prior years' March and April (T_{mean}), April (T_{min}) of the prior and current years, and December of the prior (T_{min}) temperature showed less correlation strength ($p < 0.05$) with the RWI of WHNP. Precipitation correlation

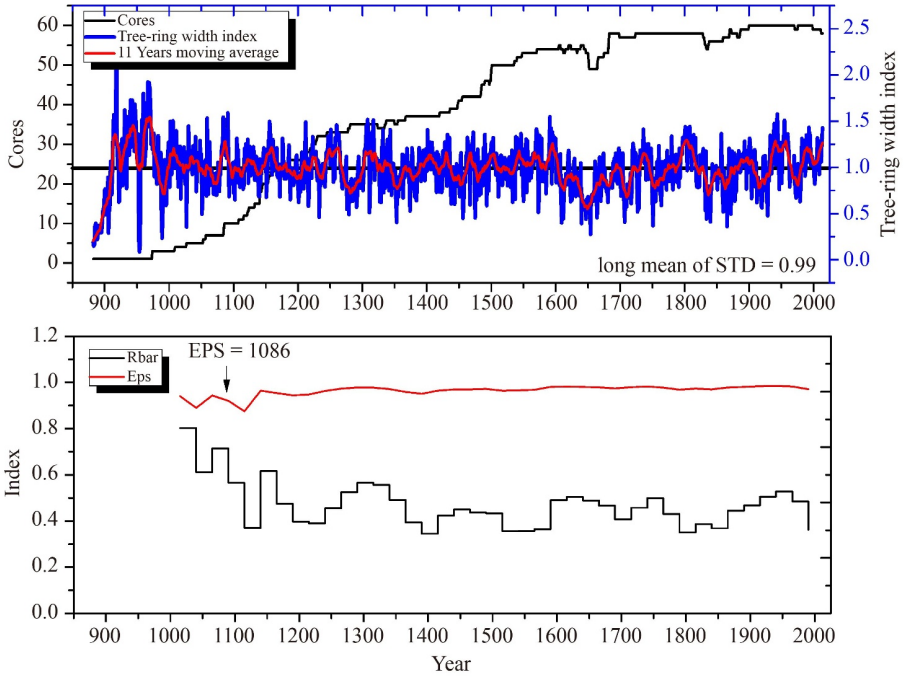

Fig. 3 Standard TRW chronology of junipers with 11-years moving average, number of tree core (upper panel), Running EPS and R-bar (lower panel). The arrow in the lower panel denotes the threshold limit (0.85).

coefficients are not significant, except in the prior year's December (r = 0.26, p < 0.05) (Fig. 4). Analysis of seasonal climate growth correlation shows that RWI is negatively and significantly correlated with summer (JJA, particularly June to July) mean temperature and insignificantly associated with winter (DJF), spring (MAM), and autumn (SON) temperatures. Similarly, RWI and precipitation are insignificantly (DJF r = 0.17; MAM r = 0.20; SON r = 0.02) and weakly (JJA r = 0.22) correlated (Fig. 4). This showed lower correlations with precipitation than with temperature, signifying that temperature is the dominant limiting factor to tree growth in this region. However, the inverse response to temperature may be interpreted as some form of moisture stress in our trees (Zafar et al., 2016). The RWI and June–July mean monthly temperature exhibit the highest association (r = −0.65, p < 0.001), which is taken into account for future analysis.

The RWI showed a statistically significant correlation the climatic parameters (p < 0.001), negative association between the RWI and temperature of June and July (Fig. 4). The negative influence of the mean monthly temperature on RWI growth is indicated by the fact that high temperatures lead to internal water deficits in the early growing season due to the increased soil moisture loss by evapotranspiration. Although the selected juniper trees are close to the high elevation treeline, their ring width showed a similar correlation pattern to tree-ring width of lower elevation spruce and pine growing on the south-facing slope (Zafar et al., 2016). This may be due to the fact that they are under the same moisture stress due to the high temperature. Therefore, it is not unexpected that there is no substantial correlation between tree growth and precipitation given the lack of rigid periodicity in precipitation, availability of snowmelt, and slope aspect. These results are consistent with the Karakoram-Himalaya (Treydte et al., 2006; Zafar et al., 2016; Khan et al., 2020; Huang et al., 2022), central Himalaya (Bhattacharyya et al., 2006; Dawadi et al., 2013) and western Himalaya and China (Cook et al., 2003; Yu et al., 2005; Bhattacharyya et al., 2006; Liang et al., 2014) that the tree growth was limited to moisture stress and negatively correlated with temperature. The *Juniperus excelsa* has a wide ecological amplitude, which is distributed in dry zones of Pakistan, e.g., (Ahmed et al., 2011). Additionally, our sample location was in northern Pakistan, which is one of the dry areas of the western Himalayas, e.g., (Treydte et al., 2006), and may be due to this phenomenon, *Juniperus excelsa* growth showed an inverse response to temperature.

3.3 Reconstruction model calibration and validation

The June–July mean monthly temperature was selected for reconstruction because of to the RWI's highly significant negative association with the mean monthly temperature during June to July. The stability of the regression model was examined using the split-period calibration and verification analysis approach (Table 2).

The calibration period of 1956–2013 C.E., the regression model explains 41.6% (R^2_{adj} = 40.6%, F = 39.90) of the measured June–July monthly mean

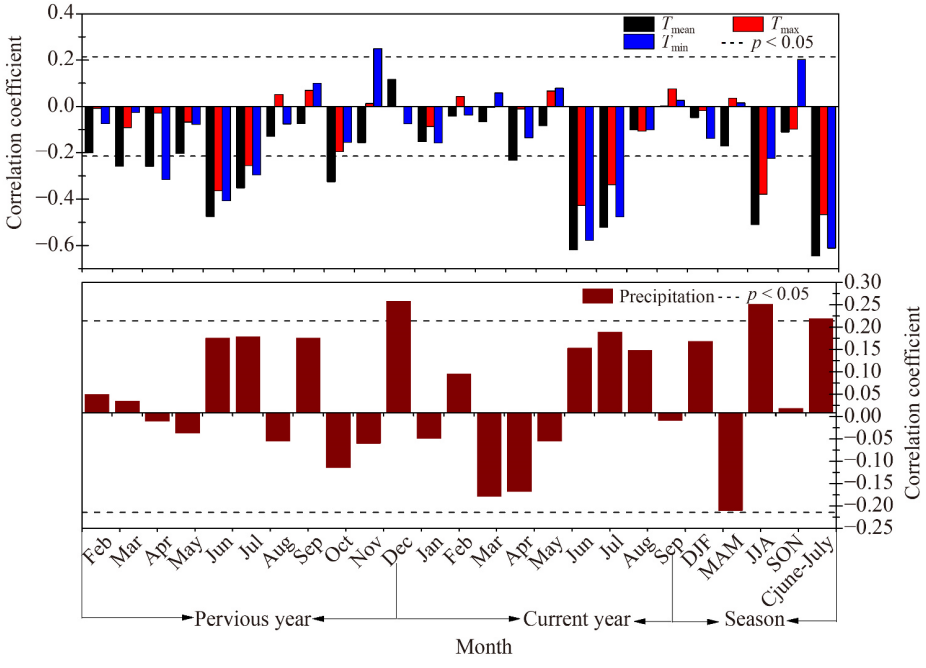

Fig. 4 Temperature (upper panel) and precipitation correlation coefficients (lower panel) between the TRW index and Bunji station data for the time span of 1955–2013. The correlations were calculated from February of the prior year to September of the current year and seasonal correlation. The black solid horizontal lines indicate a significant level with a 95% confidence interval.

temperature variance. The original data's sign tests all passed the significance test ST, $p < 0.05$), demonstrating that the model's dependability in low-frequency conditions is higher than its reliability in high-frequency situations. RE was positive for both periods of validation of 1985–2013 C.E. and 1956–1984 C.E., respectively. RE can also assume negative values when the regression estimates are especially bad in the verification period (Cook et al., 2003). A good regression model is often demonstrated by a positive RE (Cook et al., 1999). The equation $T_{\text{mean June–July}}$ = 32.44–4.43 Std, characterizing the period from 1956 to 2013 C.E., was used to reconstruct the ultimate mean June–July temperature variability back to 1086.

3.4 Reconstruction of temperature variations from 1086–2013 C.E.

The trend between the reconstructed temperature variabilities and observed data during the period 1956–2013 C.E. are consistent, whereas in magnitude showed little variation. The reconstructions of the June–July mean monthly temperature in the TRW spans the years 1086 to 2013 C.E. (Fig. 5).

The most prominent feature of the reconstruction is the warming trend in the early eighteenth and late nineteenth centuries, however it could not capture the recent warming of the twentieth century (Fig. 5). After an 11-year low pass-filter of the reconstructed temperature data, the mean temperature is 28.08°C. Based on a 1σ criteria (0.71°C) deviating from the long-term mean (28.08°C), 142 exceptionally warm and 153 extremely cold years were observed during the previous 928 years. The warmest year was observed at 1650 (30.02°C), while the coldest was the year 1261 (26.34°C). Generally, there is a 3.68°C temperature difference between the warmest years (1650, 30.02°C) and the coldest years (1261, 26.34°C). The longest warmest and coldest periods were 1637–1683

Table 2 Calibration and verification statistics of the Boibar Avgrach Valley Himalayas June–Jul mean temperature reconstruction

Statistical parameters	Calibration 1956–1984	Validation 1985–2013	Calibration 1985–2013	Validation 1956–1984	Calibration 1956–2013
r	0.676	0.404	0.410	0.677	0.645
R^2	0.456	0.164	0.168	0.458	0.416
R^2_{adj}	0.436	0.133	0.137	0.438	0.406
DW	2.005	2.475	1.515	2.010	1.691
F-value	22.673**	08.277*	6.451*	22.861**	39.904**
ST		27+/2-		26+ /3−	
RE		0.532		0.367	

Notes: r: Pearson correlation coefficient; R^2: variance explained; R^2_{adj}: adjusted variance explained; DW = Durbin–Watson statistic; ST: sign test; and RE: reduction of error; * Significant at $p = 0.01$, ** Significant at $p = 0.001$.

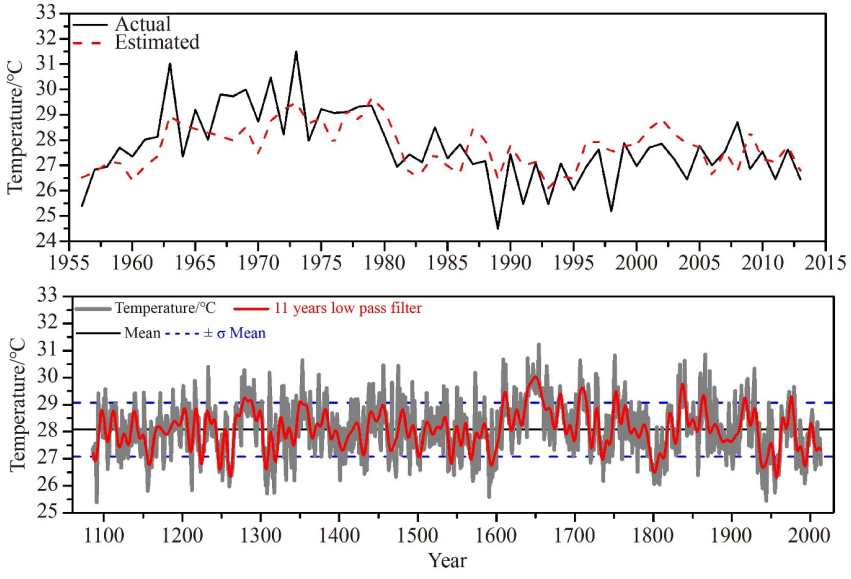

Fig. 5 Observed and estimated mean temperatures of the Himalayas during June and July for the common calibration period of 1956 to 2013 C.E. (upper panel). Reconstructed temperature from 1086 to 2013 C.E. (gray line) with an 11-year low-pass filter (red line). The horizontal center black dashed line represents the long-term mean temperature (28.08°C), while the horizontal blue-black lines (28.08 ± 1.00°C) represent the standard deviation (lower panel).

C.E. and 1796–1815 C.E. in the past 928 years, respectively (Table 3). KNMI climate explorer correlation analysis shows significant relationships ($p < 0.01$) between the June–July mean temperatures from CRU TS 4.05 and Boibar reconstruction can be seen over the Karakoram, Himalayas, West Tian Shan, Pamir, and central-east Himalaya (Fig. 6). These results suggest that the Boibar reconstruction is representative for Karakoram, Himalayas and high central Asia.

3.5 MTM spectral analysis

El Niño Southern Oscillation (ENSO) and solar activity were found to play the key role driving our regional temperature. The spectral analysis of the reconstructed mean temperature from the western Himalayas, northern displays significant ($p < 0.05$) 2–3 year and 63.8-year cycles (Fig. 7). The Multi-taper method (MTM) spectral analysis of the reconstruction displays significant ($p < 0.05$) 2–3 year and 63.8–year cycles (Fig. 6). The 2–3 years' cycle were within the range of ENSO variability, indicating the effect of ENSO on regional temperature in our study area. Similar influence of ENSO on regional temperature was also reported by nearby ice-core records on the north-western Tibetan Plateau (Yang et al., 2018) and tree rings on the central Tibetan Plateau (Liang et al., 2008). In additions, the 63.8-year cycle may be link to the solar activity. Solar radiation could influence air temperature variations through Earth rotation and atmospheric circulation (Mazzarella, 2007). Such influence of solar activity on regional temperature have also been detected on the south-eastern Tibetan Plateau (Huang et al., 2019b; Keyimu et al., 2021).

3.6 Comparison with other regional-temperature reconstructions of Pakistan

To confirm the reliability of the temperature reconstruction over a long period of time, the summer temperature series from this work was compared with other temperature series from tree rings in nearby areas (Fig. 8). The common share of cold and warm periods between the comparable reconstructions are shown in the gray shaded line, and contrasting intervals are represented by the yellow shaded line (Fig. 8). Temperature reconstruction of this study is highly consistent with the reconstructed mean June–August temperature of the Karakoram (Zafar et al., 2016) (Fig. 8, second panel). This shows that these records share common warm and cold periods on an interdecadal time scale. Our reconstructed June–July mean temperature showed a positive and significant ($r = 0.22$, $p > 0.001$) correlation with Zafar et al. (2016). The reconstructions in this study and Zafar et al. (2016) reconstruction are both based on negative correlations with summer temperatures, which may cause moisture stress rather than low-temperature limitation.

Our reconstruction showed contrasting trends with

Table 3 Extremely cold and warm periods lasting for ⩾ 4-year during AD 1086–2013

⩾ 4 year extreme cold period	⩾ 4 year extreme warm period	⩾ 4 year extreme cold period	⩾ 4 year extreme warm period
Year C.E.	Temperature/°C	Year C. E.	Temperature/°C
1276–1290	29.13 ± 0.09	1086–1092	27.08 ± 0.16
1350–1359	29.02 ± 0.06	1154–1162	27.02 ± 0.22
1453–1457	28.92 ± 0.06	1222–1227	27.06 ± 0.25
1608–1614	29.27 ± 0.17	1245–1251	26.91 ± 0.30
1637–1683	29.42 ± 0.43	1258–1264	26.69 ± 0.32
1705–1715	29.41 ± 0.21	1304–1309	26.87 ± 0.24
1750–1755	29.29 ± 0.20	1316–1321	27.10 ± 0.20
1834–1841	29.45 ± 0.28	1429–1433	27.22 ± 0.09
1861–1867	29.16 ± 0.19	1499–1504	27.17 ± 0.11
1914–1919	29.12 ± 0.13	1540–1545	27.21 ± 0.19
1973–1978	29.08 ± 0.20	1566–1570	27.08 ± 0.11
		1590–1599	26.98 ± 0.20
		1733–1738	27.14 ± 0.16
		1796–1815	26.92 ± 0.26
		1935–1947	26.96 ± 0.24
		1952–1960	26.72 ± 0.38
		1989–1996	26.98 ± 0.23

Notes: ± represents the standard deviation values of respective year's cold and warm periods. This reconstruction was obtained using the reliable chronology when the Expressed Population Signal (EPS) values of the final were higher than the standard threshold of 0.85 after 1086 C.E..

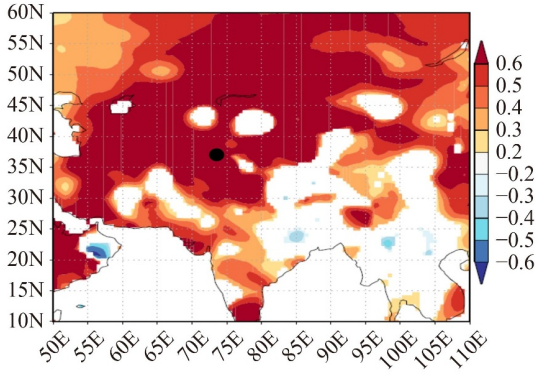

Fig. 6 Spatial correlation field of reconstructed June–July mean temperatures with gridded mean temperature from the CRU TS 4.05 data set 1955–2013. Correlation analysis was performed using the KNMI climate explorer. Black circle is the sampling site in the Himalayas northern Pakistan. Correlations are not shown if significant level $p > 0.05$.

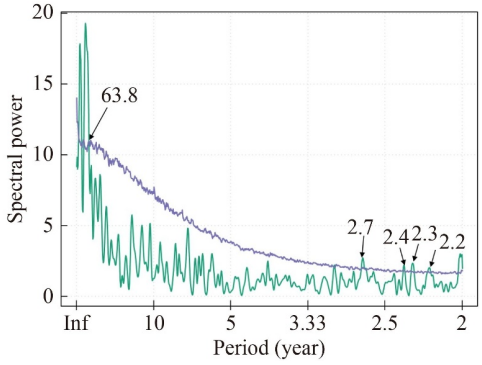

Fig. 7 Multi-taper spectrum of our temperature reconstruction and confidence intervals of 95%.

Asad et al. (2017) temperature reconstructions (Fig. 8, 3rd and 4th panel). The prior temperature reconstruction Asad et al. (2017) was based on a positive correlation mean minimum temperature and TRW, and our reconstruction was based on a negative correlation between them. The trees growth of upper treelines in the Karakoram region is limited to temperature (Asad et al., 2017), whereas our study area's forest growth is limited to high temperature related drought. Furthermore, our reconstruction failed to capture the recent warning trend of the 20th century and cold period of the Little Ice Age (1600–1900 C.E.) which was also absent in the Zafar et al. (2016) reconstruction based on negative correlation between TRW and temperature. Accordingly, we suggest that the long-term decreasing trend since 1600 may be due not indicative to temperature as the decadal to multi-decadal variations. Our reconstruction captures the pronounced cold period's Maunder minimum (1661–1663 and 1668 C.E.) and Dalton Minimum (1812–1817 and 1824–1826 C.E.), which were also reported by Khan et al. (2021) and Chen et al. (2021), and could not capture by reconstruction of Zafar et al. (2016).

4 Conclusions

We developed an 1132-year (882–2013 C.E.) TRW chronology of *Juniperus excelsa* from the western

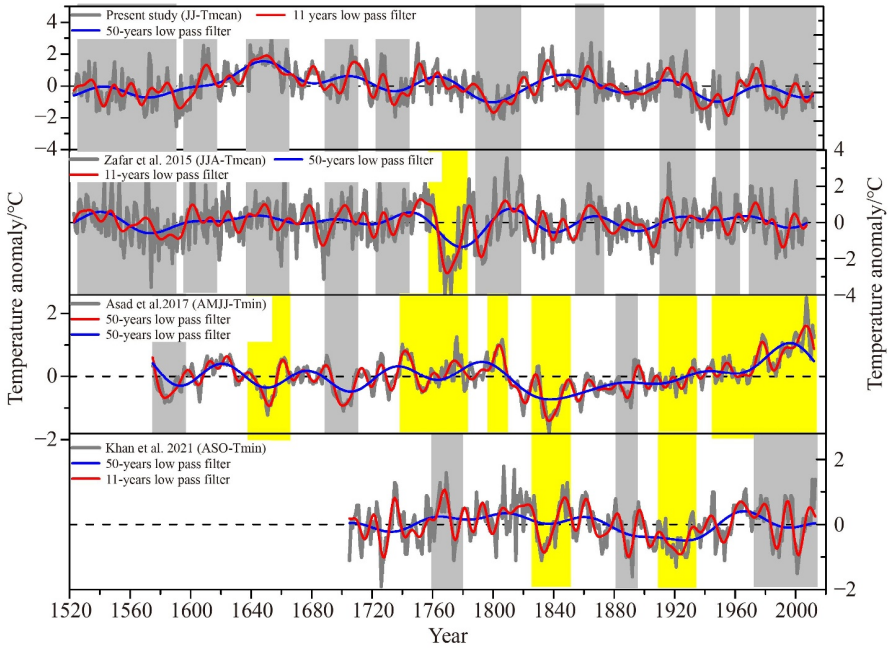

Fig. 8 Comparison of the tree-ring-based mean (JJA) and minimum (AMJJ) (Zafar et al. 2016, Asad et al. 2017). temperatures from northern Pakistan with the reconstructed mean temperature from June to July of the current study. The gray (similar trend) and yellow (inconsistent trend) shaded region depicts temperature comparisons between this research and earlier investigations in northern Pakistan.

Himalayas, northern Pakistan. The radial growth of *J. excelsa* was significantly negatively correlated ($r = -0.65$, $p > 0.001$) with the mean monthly temperature, indicating that the tree growth was mainly limited to high-temperature related drought in the western Himalayan region. Based on a strong and significant correlation, we reconstructed June to July temperatures using a robust reconstruction model over the period from 1086 to 2013. Over the previous 928 years reconstructed June–July temperature, 142 exceptionally warm years and 153 extremely cold years were observed. Our reconstruction captured the pronounced cold period's Maunder minimum and Dalton Minimum, but could not detect the recent warming trend. According to the comparison, our reconstruction is more indicative and reliable on decadal to multidecadal timescales when compared to other local temperature reconstruction series. To examine the patterns of climate change driven by global warming and to understand biological responses to climatic events, further research is needed to establish more tree-ring chronologies in the western Himalayas of northern Pakistan.

Acknowledgments We would like to thank Muhammad Zafar and Adam Khan, who kindly provided their reconstruction data for comparison. We also thank the Pakistan Metrological Department for providing the station data. A special acknowledgment should be expressed to China-Pakistan joint research center of earth sciences that supported the implementation of this study. This research was supported by the National Natural Science Foundation of China (Grant No. 42007407), the Sino-German mobility program (M-0393) and the China-Pakistan Joint Research Center on Earth Sciences (No. 131551KYSB20200022).

Competing interests The authors declare that they have no competing interests.

References

Ahmed K, Shahid S, Nawaz N (2018). Impacts of climate variability and change on seasonal drought characteristics of Pakistan. Atmos Res, 214: 364–374

Ahmed M, Palmer J, Khan N, Wahab M, Fenwick P, Esper J, Cook E (2011). The dendroclimatic potential of conifers from northern Pakistan. Dendrochronologia, 29(2): 77–88

Asad F, Zhu H, Zhang H, Liang E, Muhammad S, Farhan S B, Hussain I, Wazir M A, Ahmed M, Esper J (2017). Are Karakoram temperatures out of phase compared to hemispheric trends? Clim Dyn, 48(9–10): 3381–3390

Bhattacharyya A, Shah S K, Chaudhary V (2006). Would tree ring data of Betula utilis be potential for the analysis of Himalayan glacial fluctuations? Curr Sci, 91(6): 754–761

Bishop M P, Shroder J F Jr, Bonk R, Olsenholler J (2002). Geomorphic change in high mountains: a western Himalayan perspective. Global Planet Change, 32(4): 311–329

Bolch T, Kulkarni A, Kääb A, Huggel C, Paul F, Cogley J G, Frey H, Kargel J S, Fujita K, Scheel M, Bajracharya S, Stoffel M (2012). The state and fate of Himalayan glaciers. Science, 336(6079): 310–314

Borgaonkar H, Sabin T, Krishnan R (2020). Deciphering climate variability over western Himalaya using instrumental and tree-ring records. In: Himalayan Weather and Climate and their Impact on the Environment. New York: Springer, 205–238

Chen F, Opała-Owczarek M, Khan A, Zhang H, Owczarek P, Chen Y, Ahmed M, Chen F (2021). Late twentieth century rapid increase in high Asian seasonal snow and glacier-derived streamflow tracked by tree rings of the upper Indus River basin. Environ Res Lett, 16(9): 094055

Chhetri P (2008). Dendrochronological analyses and climate change perceptions in Langtang National Park, Central Nepal. Climate Change Disaster Impact Reduction, 28: 36–40

Cogley J G (2012). Himalayan glaciers in the balance. Nature, 488(7412): 468–469

Cook E R (1985). A Time Series Analysis Approach to Tree Ring Standardization (Dendrochronology, Forestry, Dendroclimatology, Autoregressive Process). Dissertation for Doctoral Degree. Tucson: The University of Arizona

Cook E R, Kairiukstis L A (1990). Methods of dendrochronology: applications in the environmental sciences. Springer Science & Business Media

Cook E R, Krusic P J, Jones, P D (2003). Dendroclimatic signals in long tree-ring chronologies from the Himalayas of Nepal. Intern J Climatol: J Royal Meteorol Soc, 23: 707–732

Cook E R, Meko D M, Stahle D W, Cleaveland M K (1999). Drought reconstructions for the continental United States. J Clim, 12(4): 1145–1162

Cook E, Briffa K (1990). Data analysis. In: Cook E R, Kairiukstis L A, eds. Methods of Dendrochronology: Applications in the Environmental Sciences. Dordrecht: Kluwer Academic Publishers, 97–162

Dawadi B, Liang E, Tian L, Devkota L P, Yao T (2013). Pre-monsoon precipitation signal in tree rings of timberline *Betula utilis* in the central Himalayas. Quat Int, 283: 72–77

Esper J (2000). Long-term tree-ring variations in *Juniperus* at the upper timber-line in the Karakorum (Pakistan). Holocene, 10(2): 253–260

Esper J, Frank D C, Wilson R J, Büntgen U, Treydte K (2007). Uniform growth trends among central Asian low-and high-elevation juniper tree sites. Trees (Berl), 21(2): 141–150

Esper J, Schweingruber F H, Winiger M (2002). 1300 years of climatic history for Western Central Asia inferred from tree-rings. Holocene, 12(3): 267–277

Fowler H, Archer D (2006). Conflicting signals of climatic change in the Upper Indus Basin. J Clim, 19(17): 4276–4293

Fritts H (1976). Tree Rings and Climate. New York: Academic Press

Gaire N P, Fan Z X, Shah S K, Thapa U K, Rokaya M B (2020). Tree-ring record of winter temperature from Humla, Karnali, in central Himalaya: a 229 years-long perspective for recent warming trend. Geogr Ann, Ser A, 102(3): 297–316

Hewitt K (2002). Styles of rock-avalanche depositional complexes conditioned by very rugged terrain, Karakoram Himalaya, Pakistan. Rev Eng Geol, 15: 345–377

Holmes R (1983). Computer assisted quality control. Tree-Ring Bull, 43: 69–78

Huang J G, Zhang Q B (2007). Tree rings and climate for the last 680 years in Wulan area of northeastern Qinghai-Tibetan Plateau. Clim Change, 80(3–4): 369–377

Huang R, Zhu H, Liang E, Asad F, Grießinger J (2019a). A tree-ring–based summer (June–July) minimum temperature reconstruction for the western Kunlun Mountains since AD 1681. Theor Appl Climatol, 138(1–2): 673–682

Huang R, Zhu H, Liang E, Bräuning A, Zhong L, Xu C, Feng X, Asad F, Sigdel S R, Li L, Grießinger J (2022). Contribution of winter precipitation to tree growth persists until the late growing season in the Karakoram of northern Pakistan. J Hydrol (Amst), 607: 127513

Huang R, Zhu H, Liang E, Liu B, Shi J, Zhang R, Yuan Y, Grießinger J (2019b). A tree ring-based winter temperature reconstruction for the southeastern Tibetan Plateau since 1340 CE. Clim Dyn, 53(5–6): 3221–3233

Immerzeel W W, Droogers P, De Jong S, Bierkens M (2009). Large-scale monitoring of snow cover and runoff simulation in Himalayan river basins using remote sensing. Remote Sens Environ, 113(1): 40–49

Kamp U, Owen L A (2011). Late Quaternary glaciation of northern Pakistan. In: Ehlers J, Gibbard P L, Hughes P D, eds. Quaternary Glaciations- Extent and Chronology. Develop Quat Sci, vol. 15. Elsevier, 909–927

Kargel J S, Cogley J G, Leonard G J, Haritashya U, Byers A (2011). Himalayan glaciers: the big picture is a montage. Proc Natl Acad Sci USA, 108(36): 14709–14710

Keyimu M, Li Z, Liu G, Fu B, Fan Z, Wang X, Wu X, Zhang Y, Halik U (2021). Tree-ring based minimum temperature reconstruction on the southeastern Tibetan Plateau. Quat Sci Rev, 251: 106712

Khan A, Ahmed M, Gaire N P, Iqbal J, Siddiqui M F, Khan A, Shah M, Hazrat A, Saqib N U, Mashwani W K, Shah S, Bhandari S (2021). Tree-ring-based temperature reconstruction from the western Himalayan region in northern Pakistan since 1705 CE. Arab J Geosci, 14(12): 1122

Khan A, Chen F, Ahmed M, Zafar M U (2020). Rainfall reconstruction for the Karakoram region in Pakistan since 1540 CE reveals out-of-phase relationship in rainfall between the southern and northern slopes of the Hindukush-Karakorum-Western Himalaya region. Int J Climatol, 40(1): 52–62

Kumar P, Kotlarski S, Moseley C, Sieck K, Frey H, Stoffel M, Jacob D (2015). Response of Karakoram-Himalayan glaciers to climate variability and climatic change: a regional climate model assessment. Geophys Res Lett, 42(6): 1818–1825

Liang E, Dawadi B, Pederson N, Eckstein D (2014). Is the growth of birch at the upper timberline in the Himalayas limited by moisture or by temperature? Ecology, 95(9): 2453–2465

Liang E, Shao X, Qin N (2008). Tree-ring based summer temperature reconstruction for the source region of the Yangtze River on the Tibetan Plateau. Global Planet Change, 61(3–4): 313–320

Liang E, Shao X, Xu Y (2009). Tree-ring evidence of recent abnormal warming on the southeast Tibetan Plateau. Theor Appl Climatol, 98(1–2): 9–18

Liang H, Lyu L, Wahab M (2016). A 382-year reconstruction of August mean minimum temperature from tree-ring maximum latewood density on the southeastern Tibetan Plateau, China. Dendrochronologia, 37: 1–8

Lv L X, Zhang Q B (2013). Tree-ring based summer minimum temperature reconstruction for the southern edge of the Qinghai-Tibetan Plateau, China. Clim Res, 56(2): 91–101

Mazzarella A (2007). The 60-year solar modulation of global air temperature: the Earth's rotation and atmospheric circulation connection. Theor Appl Climatol, 88(3–4): 193–199

Opała M, Niedźwiedź T, Rahmonov O, Owczarek P, Małarzewski Ł (2017). Towards improving the Central Asian dendrochronological network—new data from Tajikistan, Pamir-Alay. Dendrochronologia, 41: 10–23

Opała-Owczarek M, Niedźwiedź T, Rahmonov O, Owczarek P (2017). Millennia-long dendroclimatic records from the Pamir-Alay Mountains (Tajikistan)–perspectives and limitations. In: Wistuba M, Cedro A, Malik L, Helle G, Gärtner H, eds. TRACE–Tree Rings in Archaeology, Climatology and Ecology, Vol. 15. Scientific Technical Report 17/04. GFZ German Research Centre for Geosciences, Potsdam, Germany, 31–38

Sabin T, Krishnan R, Vellore R, Priya P, Borgaonkar H, Singh B B, Sagar A (2020). Climate change over the Himalayas. In: Krishnan R, Sanjay J, Gnanaseelan C, Mujumdar M, Kulkarni S, Chakraborty S, eds. Assessment of Climate Change over the Indian Region. New York: Springer, 207–222

Sarangzai A M, Ahmed M, Ahmed A, Tareen L, Jan S U (2012). The ecology and dynamics of *Juniperus excelsa* forest in Balochistan-Pakistan. Pak J Bot, 44: 1617–1625

Shekhar M, Bhardwaj A, Singh S, Ranhotra P S, Bhattacharyya A, Pal A K, Roy I, Martín-Torres F J, Zorzano M P (2017). Himalayan glaciers experienced significant mass loss during later phases of little ice age. Sci Rep, 7(1): 10305

Tao Q, Zhang Q B, Chen X (2021). Tree-ring reconstructed diurnal temperature range on the eastern Tibetan plateau and its linkage to El Niño-Southern Oscillation. Int J Climatol, 41(3): 1696–1711

Treydte K S, Schleser G H, Helle G, Frank D C, Winiger M, Haug G H, Esper J (2006). The twentieth century was the wettest period in northern Pakistan over the past millennium. Nature, 440(7088): 1179–1182

Wigley T M, Briffa K R, Jones P D (1984). On the average value of correlated time series, with applications in dendroclimatology and hydrometeorology. J Clim Appl Meteorol, 23(2): 201–213

Yang X, Yao T, Deji, Zhao H, Xu B (2018). Possible ENSO influences on the northwestern Tibetan Plateau revealed by annually resolved ice core records. J Geophys Res Atmos, 123(8): 3857–3870

Yu D P, Gu H Y, Wang J D, Wang Q L, Dai L M (2005). Relationships of climate change and tree ring of *Betula ermanii* tree line forest in Changbai Mountain. J For Res, 16(3): 187–192

Zafar M U, Ahmed M, Rao M P, Buckley B M, Khan N, Wahab M, Palmer J (2016). Karakorum temperature out of phase with hemispheric trends for the past five centuries. Clim Dyn, 46(5–6): 1943–1952

Zhang F, Thapa S, Immerzeel W, Zhang H, Lutz A (2019). Water

availability on the Third Pole: a review. Water Secur, 7: 100033

Zhu H F, Shao X M, Yin Z Y, Xu P, Xu Y, Tian H (2011). August temperature variability in the southeastern Tibetan Plateau since AD 1385 inferred from tree rings. Palaeogeogr Palaeoclimatol Palaeoecol, 305(1–4): 84–92

Zhu H, Huang R, Asad F, Liang E, Bräuning A, Zhang X, Dawadi B, Man W, Grießinger J (2021). Unexpected climate variability inferred from a 380-year tree-ring earlywood oxygen isotope record in the Karakoram, Northern Pakistan. Clim Dyn, 57(3–4): 701–715